A Hybrid SNN-ANN Network for Event-based Object Detection with Spatial and Temporal Attention

Soikat Hasan Ahmed[1,2], Jan Finkbeiner[1,2], and Emre Neftci[1,2]

[1] Forschungszentrum Jülich
[2] RWTH Aachen, Germany
{s.ahmed,j.finkbeiner,e.neftci}@fz-juelich.de

Abstract. Event cameras offer high temporal resolution and dynamic range with minimal motion blur, making them promising for object detection tasks. While Spiking Neural Networks (SNNs) are a natural match for event-based sensory data and enable ultra-energy efficient and low latency inference on neuromorphic hardware, Artificial Neural Networks (ANNs) tend to display more stable training dynamics and faster convergence resulting in greater task performance. Hybrid SNN-ANN approaches are a promising alternative, enabling to leverage the strengths of both SNN and ANN architectures. In this work, we introduce the first Hybrid Attention-based SNN-ANN backbone for object detection using event cameras. We propose a novel Attention-based SNN-ANN bridge module to capture sparse spatial and temporal relations from the SNN layer and convert them into dense feature maps for the ANN part of the backbone. Experimental results demonstrate that our proposed method surpasses baseline hybrid and SNN-based approaches by significant margins, with results comparable to existing ANN-based methods. Extensive ablation studies confirm the effectiveness of our proposed modules and architectural choices. These results pave the way toward a hybrid SNN-ANN architecture that achieves ANN like performance at a drastically reduced parameter budget. We implemented the SNN blocks on digital neuromorphic hardware to investigate latency and power consumption and demonstrate the feasibility of our approach.

1 Introduction

Object detection is a key and challenging problem in computer vision. It aims to recognize multiple overlapping objects and locate them in precise bounding boxes. This task has many applications in various fields, such as autonomous driving [2], medical imaging [27], and surveillance [11,45]. Over the past decade, deep learning has made significant advances in object detection. State-of-the-art approaches predominantly rely on frame-based cameras which capture frames at a fixed rate. While frame cameras offer dense intensity information, they often suffer from limited dynamic range and relatively low frame rates. Novel bio-inspired vision sensors, such as dynamic vision sensors (DVS), also known as

event cameras, are emerging as promising alternatives to conventional frame-based cameras for object detection. Event sensors operate by capturing scenes asynchronously through pixel-level illumination changes. They offer much lower latency ($\tilde{1}0\mu$ms) and higher temporal resolution and dynamic range (139 dB versus 60 dB) thereby drastically reducing motion blur. These properties are ideal for real world scenarios with low-light conditions and fast-moving objects. Despite their advantages, event-based object detection remains a relatively new area of research. Due to the sparse nature and very high temporal resolution of event-based data, effectively utilizing and efficiently processing the information-rich signal remains a challenging task in object detection pipelines.

While the fine time resolution of event cameras contains information that can be leveraged for optical flow and depth estimation, in most applications domains, the underlying causes of event data are slow compared to the temporal resolution of event sensors [43] (*e.g.* pedestrians on a street). Thus, we hypothesize that many practical vision problems can be solved by representing fast low-level spatio-temporal features in slow spatial features with no or little temporal resolution.

In this work, we used this hypothesis to create a hybrid SNN-ANN feature extractor-based architecture which combines the efficient event-driven processing of spiking neural networks (SNNs) with the powerful learning and representation capabilities of artificial neural networks (ANNs). For event-based data, many works rely mainly on well established ANN architectures [4,17,30,37,44]. ANN-based processing of event-based data provides reliable performance, but does not leverage the temporal resolution and sparsity of event-based data. SNNs, on the other hand, are ideally suited to leverage these properties at very low power and latency on an event-based neuromorphic hardware chip [3,7,36], but remain less accurate at the task level compared to ANNs. We hypothesise that a hybrid architecture including SNN and ANN processing would leverage the best of both approaches. The SNN extracts high temporal resolution low-level features of the event-based sensor into intermediate features that change on slower timescales which are then processed by the ANN. ANN processing can occur either on the edge or with reduced data rates in a cloud setting. By training the network jointly, the SNN part can leverage backpropagated errors for efficient training via the surrogate gradient approach [31].

Bridging the transition from the SNN representation to the ANN one while maintaining the essence of the spatio-temporal features is essential. To achieve this, we introduce an Attention-based SNN-ANN Bridge module. This module efficiently captures spatio-temporal spike features and transforms them into a dense feature map using two key components: Event-Rate Spatial (ERS) attention and Spatial Aware Temporal (SAT) attention. The SAT attention module addresses the challenge of sparse event inputs by enhancing the model's understanding of irregular structures. It also incorporates temporal attention to discern temporal relationships within the data. On the other hand, the ERS attention module focuses on highlighting spatial areas by leveraging the activity of events.

Related Work

Recent studies have been shedding light on the promising potential of event cameras in object detection [4, 13, 17, 23, 29, 30, 34, 34, 35, 37, 44]. In the earlier stages of adopting event cameras, the focus primarily revolved around adapting existing frame-based feature extractors along with a detection head for object detection using event data [4,17]. In [17], researchers integrated event-based data into off-the-shelf frame-based object detection networks. They employed an InceptionNet-based backbone for feature extraction and a single-shot detector (SSD) for detection [28,41]. Similarly, [34] utilized a frame-based object detection model called RetinaNet, which incorporates a spatial pooling-based feature extractor [25] along with a detection head, applied to event data. Additionally, methods such as [13,23,34] have incorporated recurrent neural networks (RNNs) as feature extractors for event data. ANN-based methods struggle to effectively utilize the temporal resolution and sparsity inherent in event-based data. [30] introduced sparse convolution as a method for event feature extraction. To address the challenges of efficiently extracting spatiotemporal features, [37] investigates the usability of a graph neural network-based approach as a feature extractor. Recently, SNN-based methods have become popular for event data processing due to their spike-based working principle, similar to event cameras, which enables efficient processing.

Research conducted by [5] and [40] showcases the effective utilization of SNNs in object detection tasks. Specifically, [5] and [40] delve into assessing the performance of converting widely-used ANN-based backbone architectures such as SqueezeNet [18], VGG [38], MobileNet [15], DenseNet [16], and ResNet [14] into SNN architecture for event-based object detection. Nonetheless, optimizing intermediate and high-level features for detection with SNNs results in a significant drop in accuracy.

Recognizing the distinct advantages offered by both SNNs and ANNs, researchers have explored merging these networks into hybrid architectures. By leveraging the complementary strengths of each, these hybrid networks show promise for simpler tasks. However, the bridge between SNNs and ANNs is still overlooked to harness the best of both worlds [20,22,22,24]. Moreover, the full extent of their capabilities remains largely unexplored, especially in tackling state-of-the-art benchmark vision tasks, such as object detection on popular datasets like Gen1 Automotive Detection dataset [8] and Gen4 Automotive Detection dataset [34].

In this paper, we addressed these problems by proposing an attention-based SNN-ANN hybrid backbone model and reporting its performance on state-of-the-art benchmark object detection datasets. Additionally, we implemented the SNN blocks in neuromorphic hardware to demonstrate the feasibility of our approach. The contributions of our work can be summarized as follows:

– A novel hybrid backbone-based event object detection model. To the best of our knowledge, this is the first work to propose a hybrid object detection approach for benchmark object detection task;

– An Attention-based SNN-ANN Bridge module featuring novel Event-Rate Spatial (ERS) attention and Spatial Aware Temporal (SAT) attention mechanisms. These mechanisms effectively bridge the SNN and ANN backbone layers;
– Implementation of the SNN blocks on digital neuromorphic hardware to validate its performance and efficiency;
– Evaluation using the publicly available benchmark datasets: Gen1 Automotive Detection dataset [8] and Gen4 Automotive Detection dataset [34]. The experimental results reveal that the proposed method outperforms the SNN-based methods while showing comparable results with the ANN-based event object detection methods.

2 Hybrid Event-based Object Detection Network

The overall hybrid network (Fig. 1) comprises two key components: an attention-based hybrid backbone designed to extract spatio-temporal features, and detection heads tasked with identifying objects. In the following section, we will delve into the details of the core components of the network.
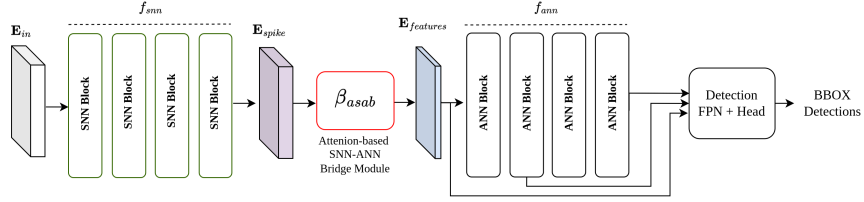

Fig. 1: Overall architecture composed of a hybrid backbone, featuring SNN blocks, attention based brdige module, and ANN blocks, and an object detection head.

Event Representation An event is represented as $e_n = (x_n, y_n, t_n, p_n)$, where (x_n, y_n) is the pixel location, t_n is the time, and p_n is polarity which indicates the change in light intensity (i.e., positive or negative). The event data is preprocessed to convert it into a time-space tensor format. Following [13], we start by creating a 4D tensor $\mathbf{E}_{in} \in \mathbb{R}^{T \times 2 \times H \times W}$, where T represents number of time discretization steps, 2 denotes polarity features which contain the count of positive and negative events in each discretized time step, and H and W signify the height and width of the event camera, respectively. Given the event set $\mathcal{E} = \{e_1, e_2, \ldots, e_N\}$, the event tensor $\mathbf{E}_{in}$ is constructed from the discretized time variable $t'_n = \left\lfloor \frac{t_n - t_a}{t_b - t_a} \cdot T \right\rfloor$ as follows:

$$\mathbf{E}_{in}(t, p, x, y) = \sum_{e_n \in \mathcal{E}} \delta\left(p - p_n\right) \delta\left(x - x_n, y - y_n\right) \delta\left(t - t'_n\right). \tag{1}$$

Attention-based Hybrid Backbone The proposed hybrid backbone architecture, as shown in Fig. 1, consists of three fundamental components: a low-level spatio-temporal feature extractor f_{snn}, an ANN-based high-level spatial feature extractor f_{ann}, and a novel Attention-based SNN-ANN Bridge (ASAB) module β_{asab}.

The first module, denoted as f_{snn}, is an event-level feature extractor operating in the spatio-temporal domain and constits of multiple SNN blocks. Each block follows a structured sequence of operations: strided convolution, batch normalization [19], and Parametric Leaky Integration and Fire (PLIF) spiking neuron [10]. The neural dynamics of PILF with trainable time constant $\tau = \text{sigmoid}(w)^{-1}$ given input $X[t]$ can be expressed as follows:

$$V[t] = V[t-1] + \frac{1}{\tau}(X[t] - (V[t-1] - V_{reset}). \tag{2}$$

The f_{snn} module receives $\mathbf{E}_{in}$ as its input and generates events $\mathbf{E}_{spike} = f_{snn}(\mathbf{E}_{in}) \in \mathbb{R}^{T \times C \times H' \times W'}$. As SNNs operate on a faster timescale and utilize sparse representations while ANNs feature dense representations, efficiently translating the valuable spatio-temporal binary spike information into dense representations is essential for obtaining effective outputs from the ANN layers. To achieve this translation, the information-rich $\mathbf{E}_{spike}$ is subsequently fed into a proposed β_{asab} module, which plays a pivotal role for the seamless integration of SNNs with ANNs. The binary spike events $\mathbf{E}_{spike}$ are converted into dense, non-binary features while preserving spatial and temporal information in the form of spatial feature maps. The output of β_{asab} is represented by $\mathbf{F}_{out} = \beta_{asab}(\mathbf{E}_{spike})$, with dimensions $C \times H' \times W'$ which is compatible with traditional 2D convolution-based networks, allowing for smooth processing and integration of information across both spatial and temporal dimensions. The attention module is further described in Sec. 2.1.

The third component, f_{ann}, extracts high-level spatial features using multiple ANN blocks with standard ANN components. Each ANN block consists of strided convolution operations, normalization [1, 19], and ReLU activation functions, enabling the extraction of detailed high-level spatial features from the densely encoded $\mathbf{F}_{out}$. The resulting outputs from the ANN blocks are then fed to the detection head for the final object detection output. More details about the architecture are provided in the supplementary material.

2.1   Attention-based SNN-ANN Bridge Module

The bridge module β_{asab} comprises two attention modules: i) Spatial-aware Temporal (SAT) attention and ii) Event-Rate Spatial (ERS) attention. The SAT attention module dynamically captures local spatial-context within the irregular spatial spike-structure to uncover temporal relations. Meanwhile, the ERS attention submodule focuses on attending to spatial areas utilizing the spatial event activities. Below, we explain these two submodules.

Spatial-aware Temporal (SAT) Attention The SAT attention contains three crucial operations: i) Channel-wise Temporal Grouping to group relevant features from different time dimensions, ii) Time-wise Separable Deformable Convolution (TSDC) denoted as Φ_{tsdc} for capturing channel-independent local spatial context from sparse spike features, and iii) Temporal attention module Φ_{ta}, which uses local spatial context features to extract temporal relations in order to accumulate and translate temporal information into spatial information.
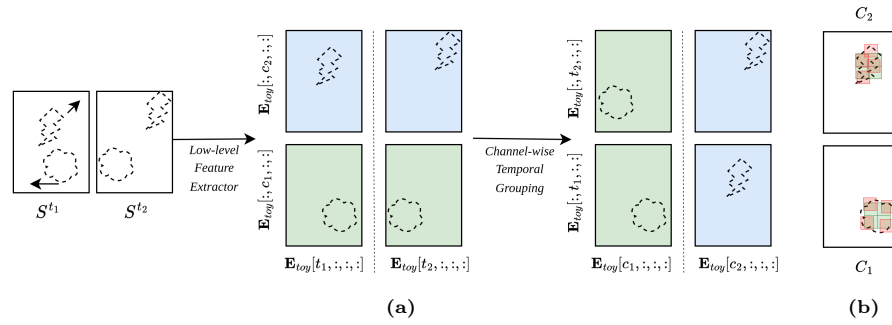

Fig. 2: Toy examples: Fig. 2a illustrates the channel-wise temporal grouping operation. In Fig. 2b, deformed kernels highlighted in red are compared with a regular grid marked in green. For visualization, a 2×2 kernel is shown as an example.

Channel-wise Temporal Grouping: Consider a scenario where two objects are moving in different directions within a scene. Since event cameras detect changes in light intensity, most events captured by the event camera in this scenario will be triggered by the edges of these objects. Additionally, due to their movements over time, there will be spatial shifting, as illustrated in Fig. 2a, denoted as S^{t1} and S^{t2}. To extract low-level features from these events, a feature extractor similar to f_{snn} processes the spatio-temporal spikes $\mathbf{E}_{toy}$, learning various features such as edges and structures across multiple channels. For illustration, consider two moving features: one round and another lightning-shaped features, as shown in the figure. We would like to group together events that are produced by one object. This can be accomplished by transposing the C and T dimensions, as illustrated in Fig. 2a. We call this procedure channel-wise temporal grouping. Note that the input and the output of the feature extractor from the input are simplified in the figure for easier understanding.

Time-wise Separable Deformable Convolution: Prior to the attention module, we apply channel-wise temporal grouping operation to the input data so that each feature channel is processed separately while capturing spatial and temporal relations. This operation transforms the input spike tensor $\mathbf{E}_{spike} \in \mathbb{R}^{T \times C \times H' \times W'}$ into $\mathbf{A}_{in} \in \mathbb{R}^{C \times T \times H' \times W'}$.

As shown in Fig. 3, the Φ_{tsdc} operation operates on individual channel-wise temporal groups $A_{in}[c_i, :, :, :]$, denoted as A_c, where i represent channel index. This operation extracts the local spatial context of the sparse, irregularly shaped spike features. This can be achieved using a deformed kernel rather than a standard square grid kernel 2b.

One important objective here is to extract spatial properties independently of the temporal dimensions. We maintain the operation as time-wise separable to prevent spatial shifts in different time dimensions from obstructing the comprehension of specific features' spatial context. The time-wise separated spatial context is then passed to the Φ_{ta} module for further processing to determine the temporal relation of different time dimensions.

For the implementation of TSDC, we utilize deformable convolution techniques introduced by [6] which adjust sampling points on the standard grid by dynamically predicting kernel offsets based on input features. During training, an additional convolutional layer called "offset learning" (refer to Fig. 3) is trained to predict these offsets. Moreover, to independently process each temporal dimension, we set the group of deformable convolution kernels equal to the number of time steps T. This approach enourages the network to focus on the spatial context of the data while maintaining temporal relations intact for further processing.
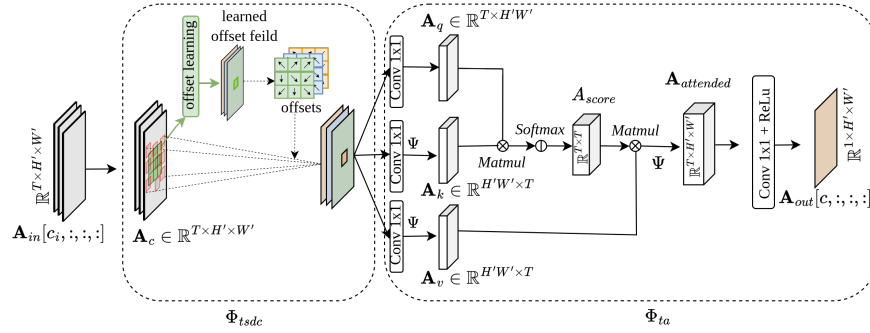

Fig. 3: Spatial-aware Temporal Attention.

Temporal Attention: To learn relationships between different time steps, we pass the local spatial context $\mathbf{A}_{sc} = \Phi_{tsdc}(A_c)$ through a temporal attention module. This module leverages the multi-head softmax self-attention mechanism introduced in [42]. In our case, we apply self-attention along the temporal dimension to extract temporal relations.

Firstly, we calculate the keys, queries, and values for temporal self-attention by employing 1×1 convolutions, followed by a reshape operation, which we denote as $\mathbf{A}_k$, $\mathbf{A}_q$, and $\mathbf{A}_v$, respectively. These operations output tensors of

shapes $\mathbb{R}^{H'W' \times T}$, $\mathbb{R}^{T \times H'W'}$, and $\mathbb{R}^{T \times H'W'}$, respectively.

$$\mathbf{A}_k = \omega_k(A_{sc}), \quad \mathbf{A}_q = \Psi(\omega_q(A_{sc})), \quad \mathbf{A}_v = Psi(\omega_v(A_{sc})) \tag{3}$$

Where Ψ denotes the reshape operation and ω denotes the 1×1 convolution operation. Next, the temporal attention scores denoted as $\mathbf{A}_{score} \in \mathbb{R}^{T \times T}$ are computed by performing matrix multiplication between $\mathbf{A}_q$ and $\mathbf{A}_k$, followed by applying a softmax operation:

$$\mathbf{A}_{score} = \mathrm{softmax}\left(\mathbf{A}_q \mathbf{A}_k\right). \tag{4}$$

To obtain the attended temporal features, we modulate the A_v by multiplying it with A_{score}, followed by a reshape operation to output $A_{attended} \in \mathbb{R}^{T \times H' \times W'}$:

$$\mathbf{A}_{attended} = \Psi(\mathbf{A}_v \mathbf{A}_{score}). \tag{5}$$

Finally, a weighted-sum along the temporal dimension using a 1×1 convolution produces the output $\mathbf{A}_{out}[c, :, :] \in \mathbb{R}^{H' \times W'}$. This operation effectively combines the attended temporal features to produce the final output.
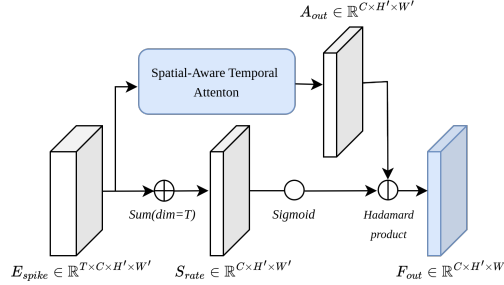

Fig. 4: Event-rate Spatial Attention.

Event-rate Spatial Attention In this attention module, we aim to extract spatial correlation as spatial weights, utilizing dynamic event activity from intermediate spikes generated by the f_{snn} module. To identify active regions, an Event-rate Spatial Attention mechanism takes the input $\mathbf{E}_{spike}$, and sums the time dimension to calculate the event rates $\mathbf{S}_{rate}$, resulting in a shape of $\mathbb{R}^{C \times H' \times W'}$: $\mathbf{S}_{rate} = \sum_{t=1}^{T} E_{spike}(t, :, :, :)$. The $\mathbf{S}_{rate}$ is first normalized using a sigmoid function to provide a spatial attention score based on the event activity. This attention score is then utilized as a weight to adjust the output of the SAT module through a Hadamard product, as visualized in Fig. 4:

$$\mathbf{F}_{out} = \mathrm{sigmoid}(\mathbf{S}_{rate}) \odot \mathbf{A}_{out} \tag{6}$$

The resulting tensor F_{out} is then fed into ANN blocks, which are subsequently utilized to predict the object detection bounding box by a detection head [12].

3 Experiments

3.1 Setup

Datasets: To conduct the training and evaluation of our network, we utilized two event-based object detection datasets: Gen1 Automotive Detection dataset [8] and Gen4 Automotive Detection dataset [34]. The Gen1 and Gen4 datasets comprise 39 and 15 hours of event camera recordings at a resolution of 304 × 240 and 720 × 1280, respectively, with bounding box annotations for car, pedestrian and two-wheeler (Gen4 only) classes.

Implementation Details: The model is implemented in PyTorch [33] and the SpikingJelly library [9]. The model is trained end-to-end over 50 epochs for the Gen 1 dataset and 10 epochs for the Gen 4 dataset. The training is performed using the ADAM optimizer [21] following a OneCycle learning rate schedule [39] with a linear decay from a maximum learning rate. The kernel size for the Φ_{tsdc} was set to 5. The training pipeline incorporates data augmentation techniques such as random horizontal flipping, zooming in, and zooming out, as outlined in [13]. Event representations for the SNN are constructed from 5 ms bins. During training, object detections are predicted every 50 ms based on the SNNs output of the last 10 time bins (50 ms). During inference, object detections can be performed at higher temporal resolution, with the timestep of the SNN setting the lower bound. For the final detection task, the YOLOX framework [12] is used, which incorporates the IOU loss, class loss, and regression loss. For Gen 1 dataset, the models are trained with a batch size of 24 and a learning rate of $2 \cdot 10^{-4}$. This training process spans approximately 8 hours and is executed on four 3090 GPUs. For the Gen 4 dataset, the batch size is set to 8 with a learning rate of $3.5 \cdot 10^{-4}$. The training duration takes around 1.5 days on four 3090 GPUs.

3.2 Comparison Results

Comparison Design To the best of our knowledge, this work presents the first hybrid object detection model which is implemented in large-scale benchmark datasets, rendering comparisons to other work challenging. Therefore, we design our comparison in three setups - (i) comparison with baseline hybrid methods, (ii) comparison with SNN-based object detection methods, and (iii) comparison with existing ANN-based methods.

Comparison Design with Baseline Method: A baseline was constructed using backbone networks similar to the proposed method. For the baseline, a VGG-11-inspired architecture [38] was adopted to maintain simplicity in the network. The proposed Attention-based SNN-ANN Bridge module was removed while keeping the input and detection heads the same as in the proposed network.

Comparison Design with SNN-based Methods: The proposed hybrid method was compared against several SNN-based methods, specifically, VGG-11+SDD [5] , MobileNet-64+SSD [5], DenseNet121-24+SSD [5], FP-DAGNet [46], EMS-RES10 [40], EMS-RES18 [40], and EMS-RES34 [40].

Comparison design with ANN-based methods: The efficacy of the proposed method was evaluated against ANN-based models, particularly, AEGNN [37], SparseConv [30], Inception + SSD [17], RRC-Events [4], Events-RetinaNet [34] and E2Vid-RetinaNet [34]. In addition, we provide comparisons with RNN-based methods such as RED [34],ASTMNet [23],RVT-B [13],RVT-S [13],RVT-T [13]. Although the performance of the ANN-based models generally outperforms models with spiking components, this comparison aims to investigate how the proposed hybrid model is comparable to the ANN models.

Evaluation Procedure: Following the evaluation protocol established in prior studies [5, 13, 34], bounding boxes with a side length of less than 10 pixels and a diagonal of less than 30 pixels were excluded for the Gen 1 dataset. Additionally, for the Gen 4 dataset, bounding boxes with a side length of less than 20 pixels and a diagonal of less than 60 pixels were eliminated. Furthermore, the input resolution was reduced to nHD resolution (640×360) for the Gen 4 dataset. The mean average precision (mAP) [26] is used as the primary evaluation metric to compare the proposed methods' effectiveness with existing approaches. Since most methods do not offer open-source code, the reported numbers from the corresponding papers were used. Tab. 1 presents a comparative analysis with

Table 1: The table presents a comparative analysis of various hybrid models for event-based object detection using metrics such as mean Average Precision (mAP) at different Intersection over Union (IoU) thresholds for two benchmark datasets.

Dataset	Models	Backbone Params	mAP(.5)	mAP(.5:.05:.95)
Gen 1	Baseline	3.3M	0.53	0.30
	Proposed	3.4M	**0.61**	**0.35**
Gen 4	Baseline	3.3M	0.47	0.26
	Proposed	3.4M	**0.50**	**0.27**

baseline methods in event-based object detection. Results show that the baseline exhibits lower mAP (.5), for instance, scoring 0.53 compared to 0.61 in Gen1, and 0.47 compared to 0.50 in Gen 4. Similarly, concerning mAP (.5:.05:.95), the baseline shows lower performance, such as 0.30 versus 0.35 in Gen1 and 0.26 versus 0.27 in Gen 4 when compared with the proposed methods. Furthermore, the proposed methods leverage irregular spatial and temporal relationships, along with event activity (i.e., rate), to discern important regions to focus on, resulting in overall improvements. The figures Fig. 5 illustrate the visual object detection

results for Gen 1 and Gen 4 datasets, respectively, in comparison with the baseline method. These visualizations demonstrate that our proposed method significantly improves the detection of smaller objects and mitigates false predictions.
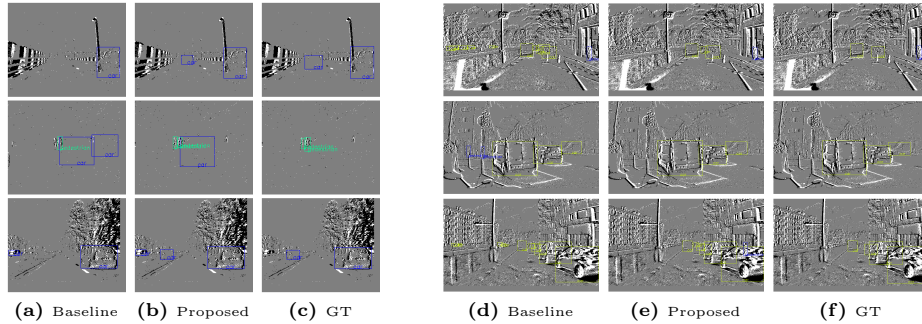

(a) Baseline **(b)** Proposed **(c)** GT   **(d)** Baseline **(e)** Proposed **(f)** GT

Fig. 5: Visual comparison with the baseline hybrid event object detection method for the Gen 1 dataset(left) and Gen 4 dataset (right). From left to right, (a,d) object detection output of the baseline method, (b,e) object detection output of the proposed method, and (c,f) ground-truth (GT) object boundaries.

Table 2: Comparative analysis of various SNN-based models for event-based object detection on the Gen1 Automotive Detection dataset [8].

Models	Type	Params	mAP(.5)	mAP(.5:.05:.95)
VGG-11+SDD [5]	SNN	13M	0.37	0.17
MobileNet-64+SSD [5]	SNN	24M	0.35	0.15
DenseNet121-24+SSD [5]	SNN	8M	0.38	0.19
FP-DAGNet [46]	SNN	22M	0.48	0.22
EMS-RES10 [40]	SNN	6.20M	0.55	0.27
EMS-RES18 [40]	SNN	9.34M	0.57	0.29
EMS-RES34 [40]	SNN	14.4M	0.59	0.31
Proposed	Hybrid	6.6M	0.61	0.35

Tab. 2 displays the comparison results with various state-of-the-art SNN-based object detection methods. It is evident from the table that our proposed method surpasses existing SNN-based methods by significant margins, despite having fewer parameters. This superiority can be attributed to our method's incorporation of a hybrid feature extraction approach with both spatial and temporal attention modules, which are lacking in other methods. Tab. 3 presents a comparison of results obtained with ANN-based event object detection models.

Table 3: Comprehensive evaluation of different ANN-based models for event-based object detection tasks on the Gen1 Automotive Detection dataset [8].

Models	Type	Params	mAP(.5:.05:.95)
RED [34]	CNN + RNN	24M	0.4
ASTMNet [23]	(T)CNN + RNN	100M	0.48
RVT-B [13]	Transformer + RNN	19M	0.47
RVT-S [13]	Transformer + RNN	10M	0.46
RVT-T [13]	Transformer + RNN	4M	0.44
AEGNN [37]	GNN	20M	0.16
SparseConv [30]	ANN	133M	0.15
Inception + SSD [17]	ANN	60M	0.3
RRC-Events [4]	ANN	100M	0.31
Events-RetinaNet [34]	ANN	33M	0.34
E2Vid-RetinaNet [34]	ANN	44M	0.27
Proposed	Hybrid	6.6M	0.35

It's worth noting that many ANN-based approaches feature a higher number of parameters. Despite incorporating SNN layers in a significant portion of our backbone, our method achieves comparable results with a smaller number of parameters. Lastly, RNN based models tend to achieve higher accuracies than the proposed hybrid network. However, two of the works, RED [34] and ASTM-Net [23] have substantially larger parameter counts and are therefore expected perform better. RVT [13] demonstrates good accuracy at a parameter count comparable to the proposed hybrid network. It is, however, based on multiple stacked transformer layers which render the overall architecture more computationally intensive due to the dynamic activation based matrix multiplications that do not contribute to the parameter count. Additionally, transformer architectures are not as straightforward to deploy on energy efficient edge computing hardware, especially neuromorphic hardware. Compared to the proposed hybrid network that is trained on 50 ms blocks, RVT has access to much longer sequences (1 s) which is hard to achieve for SNN training due to the finer grained timesteps.

3.3   Ablation Study

We performed extensive ablation studies regarding various components of the proposed ASAB module and the number of SNN and ANN blocks.

Effect of ASAB module   We constructed four variants of the proposed network, each with specific modifications. Variant 1, lacking the Ψ_{ta} operation, consistently underperforms, indicating the importance of capturing temporal relations. In Variant 2, deformable sampling is replaced with standard grid sampling, resulting in reduced accuracy due to the inability to deform and extract superior spatial context. Variant 3, without the ERS module, experiences lower accuracy

Table 4: Ablation study for ASAB module.

Models	mAP(.5)	mAP(.5:.05:.95)
Variant 1(w/o - Φta)	0.57	0.33
Variant 2 (w/o deform)	0.59	0.34
Variant 3 (w/o - ESA)	0.59	0.34
Variant 4 (Proposed)	0.61	0.35

due to the absence of spatial attention. Consequently, Variant 4, which incorporates all proposed modules, demonstrates superior performance compared to the other variants.

Effect of number of SNN blocks Three network variants were examined to assess the impact of different SNN and ANN layer numbers in the proposed architecture. The feature extractor comprised eight layers. Variant 1 decreased SNN layers and increased ANN layers in the $3-4$ setup, resulting in a slight performance boost with mAP(0.75) rising from 0.34 to 0.35. Variant 3, increasing SNN layers in the $5-3$ setup, led to reduced accuracy across all metrics due to fewer ANN layers to extract high-level features. Variant 2, utilizing the $4-4$ setting, balanced between the two, achieving comparable accuracy to Variant 1 with reduced computational overhead from additional ANN blocks. Hence, this configuration was adopted for all subsequent experiments.

Table 5: Ablation study for different settings of the number of SNN and ANN blocks. SNN - ANN represents the number of SNN and ANN blocks in the network.

Models	SNN - ANN	mAP(.5)	mAP(.75)	mAP(.5:.05:.95)
Variant 1	3 - 5	0.61	0.35	0.35
Variant 2(proposed)	4 - 4	0.61	0.34	0.35
Variant 3	5 - 3	0.58	0.33	0.33

3.4   Energy Efficiency and Hardware Implementation

In order to demonstrate the suitability of the chosen hybrid SNN-ANN approach for energy-efficient inference on the edge, we implemented the SNN backbone in hardware. In the proposed architecture the SNN block transforms sensor data into intermediate representations and therefore underlies the strictest latency requirements. Due to the clear separation between SNN and ANN parts in the model's architecture, the SNN blocks can be implemented in specialized hardware. As hardware, we chose Intel's Loihi 2 [7], a digital, programmable chip

based on event-based communication and computation. Only minor adjustments are necessary for execution on Loihi 2: The kernel-weights of the convolutional layers are quantized to `int8` via a per-output-channel quantization scheme showing no resulting loss in accuracy (mAP(.5): 0.348 (`float16`) vs 0.349 (`int8`); mAP(.5:.05:.95): 0.613 (`float16`) vs 0.612 (`int8`)). The batchnorm (BN) operations and quantization scaling are fused into the LIF-neuron dynamics by scaling and shifting the inputs according to Equations 7 and 8:

$$\text{scale} = \frac{q_{\text{scale}} \ \text{weight}_{\text{BN}}}{\tau \ \sqrt{\text{Var}_{\text{BN}} + \varepsilon_{\text{BN}}}} \tag{7}$$

$$\text{shift} = (\text{bias}_{\text{conv}} - \text{mean}_{\text{BN}}) \ \frac{\text{weight}_{\text{BN}}}{\tau \ \sqrt{\text{Var}_{\text{BN}} + \varepsilon_{\text{BN}}}} + \frac{\text{bias}_{\text{BN}}}{\tau} \tag{8}$$

where q_{scale} is the scaling factor introduced by the quantization and τ is the PLIF neurons time constant. Given this approach, spike times are almost exactly reproduced on Loihi 2 compared to the PyTorch `int8` implementation. For benchmarking purposes, the inputs to the network are simulated with an additional neuron population, due to the current IO limitations of the chip. This approach reproduces spiking statistics in the input and SNN layers.

We report power and time measurement results of the 4-layer SNN block running on Loihi 2 for inputs of size (2, 256, 160). The network runs at (1.7 ± 0.1) W and (1.9 ± 0.8) ms per step, which is faster than real-time in the currently chosen architecture (5 ms per step). These results compare favorably to commercially available chips for edge computing like the NVIDIA Jetson Orin Nano $(7\,\text{W} - 15\,\text{W})$ [32] and demonstrate the suitability of an SNN backbone for event-based data processing.

4   Conclusion

In this work, a hybrid attention-based SNN-ANN backbone for object detection using event cameras is introduced. A novel attention-based SNN-ANN bridge module is proposed to capture sparse spatial and temporal relations from the SNN layer and convert them into dense feature maps for the ANN part of the backbone. Experimental results demonstrate that our proposed method surpasses baseline hybrid and SNN-based approaches by significant margins, with results comparable to existing ANN-based methods. The efficacy of our proposed modules and architectural choices is confirmed through extensive ablation studies. Additionally, we demonstrate the effectiveness of our architectural choice with separate SNN and ANN blocks by implementing the SNN blocks on digital neuromorphic hardware, Intel's Loihi 2. The implementation achieves sub-real-time processing and improved power consumption compared to commercially available edge computing hardware. The achieved accuracy and hardware implementation results pave the way toward a hybrid SNN-ANN architecture that achieves ANN-like performance at a drastically reduced parameter and power budget.

Acknowledgement

References

1. Ba, J.L., Kiros, J.R., Hinton, G.E.: Layer normalization. arXiv preprint arXiv:1607.06450 (2016)
2. Balasubramaniam, A., Pasricha, S.: Object detection in autonomous vehicles: Status and open challenges. arXiv preprint arXiv:2201.07706 (2022)
3. Barchi, F., Urgese, G., Siino, A., Di Cataldo, S., Macii, E., Acquaviva, A.: Flexible on-line reconfiguration of multi-core neuromorphic platforms. IEEE Transactions on Emerging Topics in Computing **9**(2), 915–927 (2019)
4. Chen, N.F.: Pseudo-labels for supervised learning on dynamic vision sensor data, applied to object detection under ego-motion. In: Proceedings of the IEEE conference on computer vision and pattern recognition workshops. pp. 644–653 (2018)
5. Cordone, L., Miramond, B., Thierion, P.: Object detection with spiking neural networks on automotive event data. In: 2022 International Joint Conference on Neural Networks (IJCNN). pp. 1–8. IEEE (2022)
6. Dai, J., Qi, H., Xiong, Y., Li, Y., Zhang, G., Hu, H., Wei, Y.: Deformable convolutional networks. In: Proceedings of the IEEE international conference on computer vision. pp. 764–773 (2017)
7. Davies, M., Srinivasa, N., Lin, T.H., Chinya, G., Cao, Y., Choday, S.H., Dimou, G., Joshi, P., Imam, N., Jain, S., et al.: Loihi: A neuromorphic manycore processor with on-chip learning. Ieee Micro **38**(1), 82–99 (2018)
8. De Tournemire, P., Nitti, D., Perot, E., Migliore, D., Sironi, A.: A large scale event-based detection dataset for automotive. arXiv preprint arXiv:2001.08499 (2020)
9. Fang, W., Chen, Y., Ding, J., Yu, Z., Masquelier, T., Chen, D., Huang, L., Zhou, H., Li, G., Tian, Y.: Spikingjelly: An open-source machine learning infrastructure platform for spike-based intelligence. Science Advances **9**(40), eadi1480 (2023)
10. Fang, W., Yu, Z., Chen, Y., Masquelier, T., Huang, T., Tian, Y.: Incorporating learnable membrane time constant to enhance learning of spiking neural networks. In: Proceedings of the IEEE/CVF International Conference on Computer Vision (ICCV). pp. 2661–2671 (October 2021)
11. Fleck, T., Pavlitska, S., Nitzsche, S., Pachideh, B., Peccia, F., Ahmed, S.H., Meyer, S.M., Richter, M., Broertjes, K., Neftci, E., et al.: Low-power traffic surveillance using multiple rgb and event cameras: A survey. In: 2023 IEEE International Smart Cities Conference (ISC2). pp. 1–7. IEEE (2023)
12. Ge, Z., Liu, S., Wang, F., Li, Z., Sun, J.: Yolox: Exceeding yolo series in 2021. arXiv preprint arXiv:2107.08430 (2021)
13. Gehrig, M., Scaramuzza, D.: Recurrent vision transformers for object detection with event cameras. In: Proceedings of the IEEE/CVF Conference on Computer Vision and Pattern Recognition. pp. 13884–13893 (2023)
14. He, K., Zhang, X., Ren, S., Sun, J.: Deep residual learning for image recognition. In: Proceedings of the IEEE conference on computer vision and pattern recognition. pp. 770–778 (2016)

15. Howard, A.G., Zhu, M., Chen, B., Kalenichenko, D., Wang, W., Weyand, T., Andreetto, M., Adam, H.: Mobilenets: Efficient convolutional neural networks for mobile vision applications. arXiv preprint arXiv:1704.04861 (2017)
16. Huang, G., Liu, Z., Van Der Maaten, L., Weinberger, K.Q.: Densely connected convolutional networks. In: Proceedings of the IEEE conference on computer vision and pattern recognition. pp. 4700–4708 (2017)
17. Iacono, M., Weber, S., Glover, A., Bartolozzi, C.: Towards event-driven object detection with off-the-shelf deep learning. In: 2018 IEEE/RSJ International Conference on Intelligent Robots and Systems (IROS). pp. 1–9. IEEE (2018)
18. Iandola, F.N., Han, S., Moskewicz, M.W., Ashraf, K., Dally, W.J., Keutzer, K.: Squeezenet: Alexnet-level accuracy with 50x fewer parameters and< 0.5 mb model size. arXiv preprint arXiv:1602.07360 (2016)
19. Ioffe, S., Szegedy, C.: Batch normalization: Accelerating deep network training by reducing internal covariate shift. In: International conference on machine learning. pp. 448–456. pmlr (2015)
20. Johansson, O.: Training of object detection spiking neural networks for event-based vision (2021)
21. Kingma, D.P., Ba, J.: Adam: A method for stochastic optimization. arXiv preprint arXiv:1412.6980 (2014)
22. Lee, C., Kosta, A.K., Zhu, A.Z., Chaney, K., Daniilidis, K., Roy, K.: Spike-flownet: event-based optical flow estimation with energy-efficient hybrid neural networks. In: European Conference on Computer Vision. pp. 366–382. Springer (2020)
23. Li, J., Li, J., Zhu, L., Xiang, X., Huang, T., Tian, Y.: Asynchronous spatio-temporal memory network for continuous event-based object detection. IEEE Transactions on Image Processing **31**, 2975–2987 (2022)
24. Lien, H.H., Chang, T.S.: Sparse compressed spiking neural network accelerator for object detection. IEEE Transactions on Circuits and Systems I: Regular Papers **69**(5), 2060–2069 (2022)
25. Lin, T.Y., Dollár, P., Girshick, R., He, K., Hariharan, B., Belongie, S.: Feature pyramid networks for object detection. In: Proceedings of the IEEE conference on computer vision and pattern recognition. pp. 2117–2125 (2017)
26. Lin, T.Y., Maire, M., Belongie, S., Hays, J., Perona, P., Ramanan, D., Dollár, P., Zitnick, C.L.: Microsoft coco: Common objects in context. In: Computer Vision–ECCV 2014: 13th European Conference, Zurich, Switzerland, September 6-12, 2014, Proceedings, Part V 13. pp. 740–755. Springer (2014)
27. Litjens, G., Kooi, T., Bejnordi, B.E., Setio, A.A.A., Ciompi, F., Ghafoorian, M., Van Der Laak, J.A., Van Ginneken, B., Sánchez, C.I.: A survey on deep learning in medical image analysis. Medical image analysis **42**, 60–88 (2017)
28. Liu, W., Anguelov, D., Erhan, D., Szegedy, C., Reed, S., Fu, C.Y., Berg, A.C.: Ssd: Single shot multibox detector. In: Computer Vision–ECCV 2016: 14th European Conference, Amsterdam, The Netherlands, October 11–14, 2016, Proceedings, Part I 14. pp. 21–37. Springer (2016)
29. Maass, W.: Networks of spiking neurons: the third generation of neural network models. Neural networks **10**(9), 1659–1671 (1997)
30. Messikommer, N., Gehrig, D., Loquercio, A., Scaramuzza, D.: Event-based asynchronous sparse convolutional networks. In: Computer Vision–ECCV 2020: 16th European Conference, Glasgow, UK, August 23–28, 2020, Proceedings, Part VIII 16. pp. 415–431. Springer (2020)
31. Neftci, E.O., Mostafa, H., Zenke, F.: Surrogate gradient learning in spiking neural networks: Bringing the power of gradientbased optimization to spiking

neural networks. IEEE Signal Processing Magazine **36**(6),   5163 (Nov 2019). https://doi.org/10.1109/MSP.2019.2931595, https://ieeexplore.ieee.org/ielaam/79/8887548/8891809aam.pdf

32. NVIDIA Corporation: Jetson orin nano series modules data sheet. https://developer.download.nvidia.com/assets/embedded/secure/jetson/orin_nano/docs/Jetson-Orin-Nano-Series-Modules-Data-Sheet_DS-11105-001 _ v1 . 2 . pdf ? ZrWsxOuNKtqCuiRjutBiAvgpv1iVAHXTOGPHxDTfivnHUgfE8 _ QRTfEvfAy7RmSKTjchWhMOwfclEabwKjRuJY9CcOywW_   - 0voQ6KNLb9D5zdSkuj1jz4CClwzqrbcT5dDaA6YD8c7GLGs5ami9KVyHZp4aDpxHakdQJlg9qqfmprespOFvkMAcs1_ gVIzxcxX1ZaixLRpubBckJ5uXf69Yz1JkIeua9xYmcLA   =   =   &   t   = eyJscyI6ImdzZW8iLCJsc2QiOiJodHRwczovL3d3dy5nb29nbGUuY29tLy,   accessed: March 7, 2024

33. Paszke, A., Gross, S., Massa, F., Lerer, A., Bradbury, J., Chanan, G., Killeen, T., Lin, Z., Gimelshein, N., Antiga, L., et al.: Pytorch: An imperative style, high-performance deep learning library. Advances in neural information processing systems **32** (2019)

34. Perot, E., De Tournemire, P., Nitti, D., Masci, J., Sironi, A.: Learning to detect objects with a 1 megapixel event camera. Advances in Neural Information Processing Systems **33**, 16639–16652 (2020)

35. Roy, K., Jaiswal, A., Panda, P.: Towards spike-based machine intelligence with neuromorphic computing. Nature **575**(7784), 607–617 (2019)

36. Sawada, J., Akopyan, F., Cassidy, A.S., Taba, B., Debole, M.V., Datta, P., Alvarez-Icaza, R., Amir, A., Arthur, J.V., Andreopoulos, A., et al.: Truenorth ecosystem for brain-inspired computing: scalable systems, software, and applications. In: SC'16: Proceedings of the International Conference for High Performance Computing, Networking, Storage and Analysis. pp. 130–141. IEEE (2016)

37. Schaefer, S., Gehrig, D., Scaramuzza, D.: Aegnn: Asynchronous event-based graph neural networks. In: Proceedings of the IEEE/CVF conference on computer vision and pattern recognition. pp. 12371–12381 (2022)

38. Simonyan, K., Zisserman, A.: Very deep convolutional networks for large-scale image recognition. arXiv preprint arXiv:1409.1556 (2014)

39. Smith, L.N., Topin, N.: Super-convergence: Very fast training of neural networks using large learning rates. In: Artificial intelligence and machine learning for multi-domain operations applications. vol. 11006, pp. 369–386. SPIE (2019)

40. Su, Q., Chou, Y., Hu, Y., Li, J., Mei, S., Zhang, Z., Li, G.: Deep directly-trained spiking neural networks for object detection. In: Proceedings of the IEEE/CVF International Conference on Computer Vision. pp. 6555–6565 (2023)

41. Szegedy, C., Liu, W., Jia, Y., Sermanet, P., Reed, S., Anguelov, D., Erhan, D., Vanhoucke, V., Rabinovich, A.: Going deeper with convolutions. In: Proceedings of the IEEE conference on computer vision and pattern recognition. pp. 1–9 (2015)

42. Vaswani, A., Shazeer, N., Parmar, N., Uszkoreit, J., Jones, L., Gomez, A.N., Kaiser, Ł., Polosukhin, I.: Attention is all you need. Advances in neural information processing systems **30** (2017)

43. Wiskott, L., Sejnowski, T.J.: Slow feature analysis: Unsupervised learning of invariances. Neural computation **14**(4), 715770 (2002)

44. Yik, J., Ahmed, S.H., Ahmed, Z., Anderson, B., Andreou, A.G., Bartolozzi, C., Basu, A., Blanken, D.d., Bogdan, P., Bohte, S., et al.: Neurobench: Advancing neuromorphic computing through collaborative, fair and representative benchmarking. arXiv preprint arXiv:2304.04640 (2023)

45. Zhang, C., Kim, J.: Object detection with location-aware deformable convolution and backward attention filtering. In: Proceedings of the IEEE/CVF Conference on Computer Vision and Pattern Recognition. pp. 9452–9461 (2019)
46. Zhang, H., Leng, L., Che, K., Liu, Q., Cheng, J., Guo, Q., Liao, J., Cheng, R.: Automotive object detection via learning sparse events by temporal dynamics of spiking neurons. arXiv preprint arXiv:2307.12900 (2023)

Supplementary Materials for
A Hybrid SNN-ANN Network for Event-based Object Detection with Spatial and Temporal Attention

Soikat Hasan Ahmed[1,2], Jan Finkbeiner[1,2], and Emre Neftci[1,2]

[1] Forschungszentrum Jülich
[2] RWTH Aachen, Germany
{s.ahmed,j.finkbeiner,e.neftci}@fz-juelich.de

Abstract. Event cameras offer high temporal resolution and dynamic range with minimal motion blur, making them promising for object detection tasks. While Spiking Neural Networks (SNNs) are a natural match for event-based sensory data and enable ultra-energy efficient and low latency inference on neuromorphic hardware, Artificial Neural Networks (ANNs) tend to display more stable training dynamics and faster convergence resulting in greater task performance. Hybrid SNN-ANN approaches are a promising alternative, enabling to leverage the strengths of both SNN and ANN architectures. In this work, we introduce the first Hybrid Attention-based SNN-ANN backbone for object detection using event cameras. We propose a novel Attention-based SNN-ANN bridge module to capture sparse spatial and temporal relations from the SNN layer and convert them into dense feature maps for the ANN part of the backbone. Experimental results demonstrate that our proposed method surpasses baseline hybrid and SNN-based approaches by significant margins, with results comparable to existing ANN-based methods. Extensive ablation studies confirm the effectiveness of our proposed modules and architectural choices. These results pave the way toward a hybrid SNN-ANN architecture that achieves ANN-like performance at a drastically reduced parameter budget. We implemented the SNN blocks on digital neuromorphic hardware to investigate latency and power consumption and demonstrate the feasibility of our approach.

1 Supplementary Details

The supplementary material accompanies the manuscript titled "A Hybrid SNN-ANN Network for Event-based Object Detection with Spatial and Temporal Attention" and includes the architecture details of the proposed hybrid backbone network as well as hardware performance details.

1.1 Network Architecture

Tab. 1 displays the network architecture of the proposed hybrid backbone. Additionally, Fig. 1 illustrates the basic SNN and ANN blocks. For better understand-

ing, we have also included an additional figure (Fig. 2) to clarify the channel-wise temporal grouping operation from Spatial-aware Temporal attention, where similar features from different time dimensions are grouped.
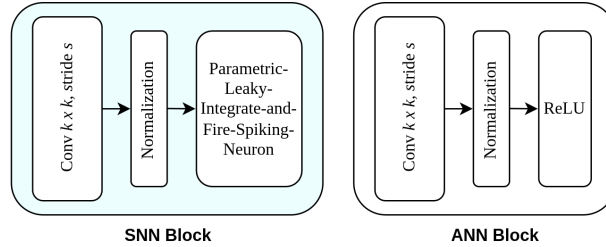

Fig. 1: Basic SNN and ANN blocks.

Table 1: Hybrid backbone architecture, where the kernel $XcKpZsS$ represents X convolution filters of size $K \times K$ with padding Z and stride S.

Layer	Kernel	Output Dimensions	Layer Type
Input	-	$T \times 2 \times H \times W$	
1	$64c3p1s2$	$T \times 64 \times \frac{1}{2}H \times \frac{1}{2}W$	
2	$128c3p1s2$	$T \times 128 \times \frac{1}{4}H \times \frac{1}{4}W$	SNN Layers
3	$256c3p1s2$	$T \times 256 \times \frac{1}{8}H \times \frac{1}{8}W$	
4	$256c3p1s1$	$T \times 256 \times \frac{1}{8}H \times \frac{1}{8}W$	
5	-	$256 \times \frac{1}{8}H \times \frac{1}{8}W$	$\beta asab$
6	$256c3p1s1$	$256 \times \frac{1}{8}H \times \frac{1}{8}W$	
7	$256c3p1s2$	$256 \times \frac{1}{16}H \times \frac{1}{16}W$	ANN Layers
8	$256c3p1s1$	$256 \times \frac{1}{16}H \times \frac{1}{16}W$	
9	$256c3p1s2$	$256 \times \frac{1}{32}H \times \frac{1}{32}W$	
		Detection Head YoloX [2]	

1.2 Hardware Implementation

This section provides more performace details on the hardware implementation of the spiking layers of the backbone on a digital neuromorphic chip, Intel's Loihi 2 [1]. In Tab. 3, we present the Power and time measurements of the SNN block on Loihi 2 for various input sizes, each tested with different weight quantization settings.
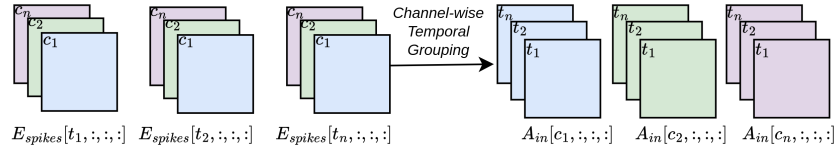
Fig. 2: Visualization of channel-wise temporal grouping.

Table 2: This table shows the effects of accuracy due to the quantization of the weights for the SNN blocks, aimed at making them compatible with neuromorphic hardware.

Models	mAP(.5)	mAP(.5:.05:.95)
Variant 1 (float16)	0.613	0.348
Variant 2 (int8)	0.612	0.349
Variant 3 (int6)	0.612	0.348
Variant 4 (int4)	0.610	0.347
Variant 5 (int2)	0.432	0.224

References

1. Davies, M., Srinivasa, N., Lin, T.H., Chinya, G., Cao, Y., Choday, S.H., Dimou, G., Joshi, P., Imam, N., Jain, S., et al.: Loihi: A neuromorphic manycore processor with on-chip learning. Ieee Micro **38**(1), 82–99 (2018)
2. Ge, Z., Liu, S., Wang, F., Li, Z., Sun, J.: Yolox: Exceeding yolo series in 2021. arXiv preprint arXiv:2107.08430 (2021)

Table 3: Power and time measurements of the SNN block on Loihi 2 for several input sizes and number of weight bits. The power is measured in Watts and the execution time per step in milliseconds. The mean and standard deviation of the measurements averaged over 12 inputs for a total of 100k steps are reported.

Input size (C,W,H)	Weight qunatization	Number of chips	Total Power [W]	Execution Time Per Step [ms]
	int8	6	1.73 ± 0.10	2.06 ± 0.74
(2, 256, 160)	int6	6	1.71 ± 0.11	2.06 ± 0.74
	int4	6	1.95 ± 0.33	1.16 ± 0.49
	int8	4	1.51 ± 0.56	0.80 ± 0.32
(2, 128, 160)	int6	4	1.81 ± 0.48	0.45 ± 0.18
	int4	3	1.39 ± 0.44	0.49 ± 0.18